JOURNAL OF MATERIALS SCIENCE 30 (1995) 308–320

Review
Atomic oxygen resistant coatings for low earth orbit space structures

S. PACKIRISAMY*, D. SCHWAM, M. H. LITT
Department of Macromolecular Science, Case Western Reserve University, Cleveland, Ohio 44106, USA

This review presents research in the area of polymeric coatings developed for protecting low earth orbit (LEO) space structures from atomic oxygen. Following a brief description of the LEO environment, ground-based simulation facilities for atomic oxygen and evaluation of protective coatings are discussed. Atomic oxygen resistant coatings based on different polymeric systems such as fluorinated polymers, silicones, poly(carborane–siloxane)s and decarborane-based polymers are presented. Finally, the performances of different coating systems are compared and the scope for further research to improve the performance of some of the coating systems is discussed.

1. Introduction

In recent years, the emphasis in space research has been shifting from space exploration to commercialization of space. In order to utilize space for commercial purposes it is necessary to understand the low earth orbit (LEO) space environment where most of the activities will be carried out. Studies on the LEO environment are mainly focused towards understanding: (i) the effect of atomic oxygen on spacecraft materials, (ii) the effect of micrometeroid and debris impact, and (iii) the effect of far ultraviolet (u.v.) hard radiation and particles generally. The spacecraft materials in LEO are vulnerable to the combined effects of thermal cycling, far u.v. radiation, high-vacuum, micrometeroid and debris impact, charged particle bombardment, spacecraft charging and atomic oxygen [1].

Atomic oxygen formed by the photodissociation of molecular oxygen in the upper atmosphere is the most severe threat to a space station in LEO

$$O_2 + h\nu \rightarrow O\cdot + O\cdot \ (99\%)$$
$$O^+ + O^- \ (\ll 1\%)$$

The high orbital velocity of 8 $km\,s^{-1}$ accelerates degradation by increasing the energy of the atomic oxygen impact with the spacecraft surface.

Advanced composites and engineering thermoplastic materials are strong candidates for construction materials for space stations due to their high specific strength. However, all carbon-based materials degrade rapidly in contact with atomic oxygen [2–5]. Degradation of the organic matrix could easily expose glass fibres which would contaminate the space station environment. A Kapton© (polyimide) blanket several mm thick serves as a support and as a radiative heat sink for the photovoltaic arrays. A 2 mm (50 μm) thick Kapton© blanket, for instance, would completely erode within 6 months. The solar cells would fail much sooner from overheating as surface roughening of the blanket reduces radiative cooling. Silver used in solar thermal power systems reacts with atomic oxygen faster than Kapton©. Thus, structures in the LEO environment require protective coatings.

There have been several approaches to protective coatings for atomic oxygen. Metal oxide coatings have negligible erosion rates since they are completely oxidized already. The coatings, however, lack flexibility, require elaborate sputtering techniques for application on complex shapes, and are susceptible to pinhole defects caused by shadowing dust particles. They also crack easily on thermal cycling since the substrates, usually polymers, have much higher thermal expansion coefficients.

Of late, attention has been focused on the use of polymeric materials as protective coatings for atomic oxygen. Fluorinated polymers, silicones, poly(carborane–siloxane)s and decaborane-based polymers have been considered for this purpose. The ease and flexibility of application by spin-coating, dip-coating or spraying allows the coating of flexible structures or complex shapes.

The objective of this paper is to present a critical overview of recent developments in the use of polymeric materials as atomic oxygen resistant coatings for LEO space structures. The selection of a suitable coating material involves the evaluation of various coatings in a ground-based LEO simulation facility. In recent years a great deal of research has been put into simulating the LEO environment and developing

* *Present address*: Vikram Sarabhi Space Centre, Trivandrum 695 002, India.

0022–2461

suitable testing and evaluation procedures for coatings exposed to atomic oxygen. Following a brief description of developments in these areas, the use of polymeric materials such as fluorinated polymers, silicones, poly(carborane–siloxane)s and decaborane-based polymers as atomic oxygen resistant coatings are discussed. Finally, different coating systems are compared and the scope for further research is outlined.

2. LEO environment

In order to develop protective coatings for space structures used in the LEO environment it is necessary to understand this environment with particular reference to atomic oxygen. This section presents a brief overview of the factors which influence the atomic oxygen concentration.

Atomic oxygen is the most prevalent species in the upper atmosphere from 200 to 700 km (Fig. 1) [6–8]. At orbital altitude the neutral atmosphere consists primarily of 80% atomic oxygen and 20% molecular nitrogen.

Since atomic oxygen is formed by photodissociation, its concentration depends strongly on solar activity and position [9]. Diurnal variations of atomic oxygen density in the upper atmosphere result from the earth's rotation about its axis. During rotation, regions of the atmosphere illuminated by the sun are warmed by its rays and regions in darkness are cooled by radiative heat loss to space. These variations become more pronounced at higher altitudes. During conditions of high solar activity, the dayside density at 600 km altitude may be a factor of 8 higher than the nightside density.

The atomic oxygen number density varies from 10^9 to 10^8 atoms cm^{-3} over an altitude range of 300–500 km during conditions of high solar activity. With low solar activity, concentrations over these altitudes are reduced to 10^8–10^6 atoms cm^{-3} (Fig. 2) [10]. Consequently, a spacecraft launched during times of minimum solar activity experiences less exposure to atomic oxygen than one launched during times of high activity. Typically, a space shuttle mission which is flown at an altitude near 300 km would encounter an average atomic oxygen density between 10^8 and 10^9 atoms cm^{-3} during the 11-year solar cycle. Spacecraft

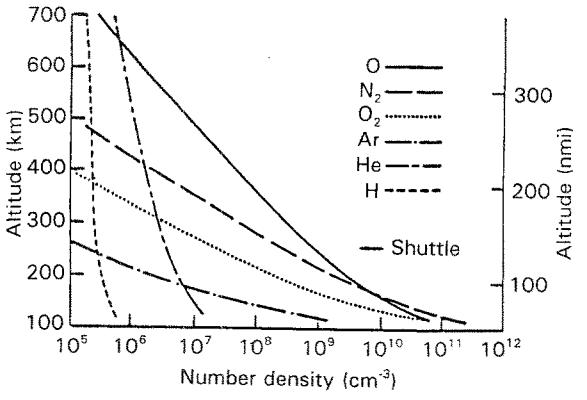

Figure 1 Atmospheric composition as a function of altitude (adapted from Purvis [7]).

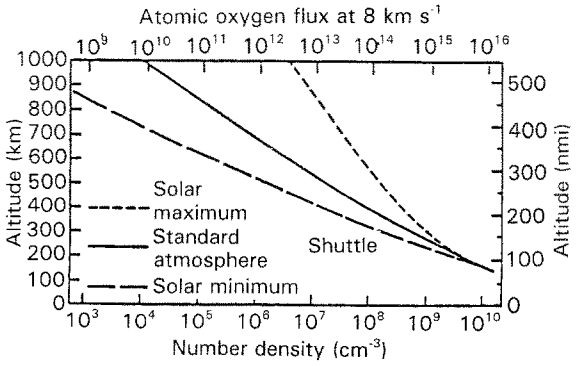

Figure 2 Atomic oxygen density as a function of altitude and solar cycle intensity (adapted from Tenny [10]).

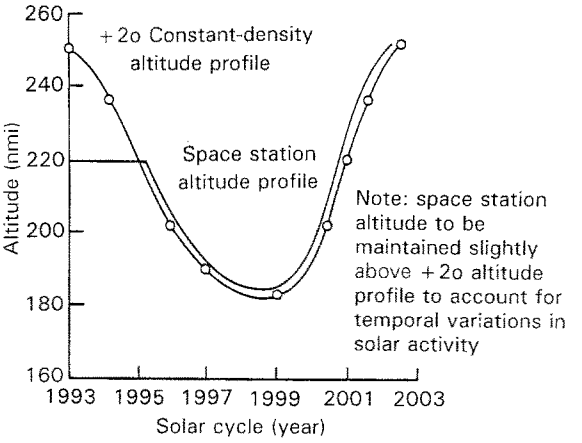

Figure 3 Variable altitude strategy for space station freedom (adapted from Visentine [9]).

flown at a higher altitude of 500 km would encounter much lower number densities (10^6–10^8 atoms cm^{-3}) over the same exposure period.

The expansion of the atmosphere during conditions of high solar activity causes a substantial increase of drag on the spacecraft surfaces. To reduce the space transportation system (STS) operating costs and decrease the effects on space-station microgravity experiments, NASA has opted to vary the station's altitude to keep the atmosphere atom density constant [9]. The altitude profile is shown in Fig. 3. The altitude will vary from 180 nautical miles (nmi) (300 km) during low activity to 225 nmi (375 km) during high solar activity. This variable altitude strategy will require fewer shuttle resupply flights because more cargo can be put into orbit during periods when the station is at lower altitudes. This approach will, however, increase the atomic oxygen effect on the station fourfold. Thus, when compared to a constant altitude strategy, the need for protective coatings to limit atomic oxygen surface interactions becomes even more urgent.

3. Effect of atomic oxygen on polymeric materials

Early space missions such as STS-5, STS-8 and STS-41G showed that materials exposed to the flight environment undergo changes. Surface erosion as high as

0.5 μm per orbit has occurred for organic materials [9]. Some metals, notably osmium and silver, became heavily oxidized in the LEO environment.

Surfaces facing the flight direction (ram oriented) encounter atomic oxygen with a relative kinetic energy of 4–5 eV (Fig. 4) [7, 11] depending on the orbital velocity. Atomic oxygen may initiate numerous chemical and physical events on the surface it impacts; it may simply be scattered or it may react chemically with nitrogen, also incident upon the surface to form nitric oxide in an excited state, which can de-excite to produce a glow. If atomic oxygen reacts with an organic material, volatile fragments, such as short-chain oxidation products, may leave the surface. The surface may also be populated with excited state fragments, radicals or polymeric molecules with oxygen-containing functionalities. The oxygen may also, as in the case of silver, diffuse into the bulk of the material (Fig. 5) [12].

The atomic oxygen interaction with materials can be quantified by measurement of atomic oxygen flux and multiplying it by the duration of exposure, which results in an atomic oxygen effect in terms of atoms per square cm. The recession of material is usually measured in terms of weight or volume. The chemistry of the remaining or reacted surface may be analysed by surface analysis, optical characterization and mechanical characterization (in terms of modulus of elasticity and brittleness).

Atomic oxygen exposure of various polymeric materials, metals and inorganic materials permits the calculation of erosion yield, which is defined as the volume of material lost per oxygen atom; the values are presented in Table I [12, 13]. Based upon the evaluation of materials in space, there appear to be three classes of materials:

(a) materials of high erosion yield, which include most of the hydrocarbon organic materials
(b) materials which either do not react with atomic oxygen or form self-protecting oxide coatings so that the underlying materials are durable to atomic oxygen

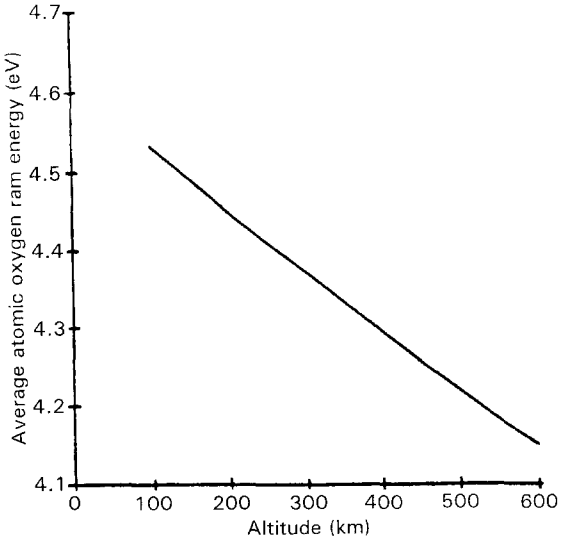

Figure 4 Variation of atomic oxygen energy with altitude (adapted from Banks *et al.* [11]).

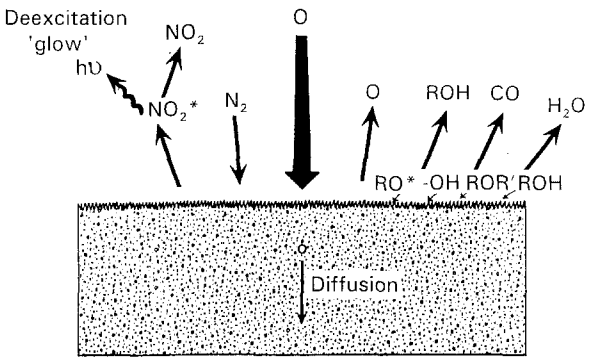

Figure 5 Interaction of atomic oxygen with organic materials (adapted from Banks *et al.* [12]).

TABLE I Erosion yield of various materials exposed to LEO environment

Material	Erosion yield $\times 10^{-24}$ cm^{-3} atom^{-1}
Aluminium	0.00
Al_2O_3	< 0.025
Carbon	1.2
Diamond	0.021
Epoxy	1.7
Gold	0.0
Graphite epoxy	2.6
Kapton	3.0
Polyethylene	3.3
Poly(methylacrylate)	3.4
Polycarbonate	6.0
Polystyrene	1.7
Polysulfone	2.4
Silicone	0.05
Siloxane polyimide (7%Sx)	0.6
Siloxane polyimide (25%Sx)	0.3
Poly(vinylfluoride)	3.2
Polytetrafluoroethylene	0.03–0.5

(c) materials with low, but non-negligible erosion yields, such as fluoropolymers.

In the LEO environment, materials with high erosion yields should either not be used or be protected by coating with materials having negligible erosion yields.

4. LEO atomic oxygen simulation

To facilitate accurate prediction of materials performance in the LEO, one must be able to simulate LEO environmental conditions accurately, or at least be able to extrapolate quantifiably how the performance of materials under simulated conditions relates to that which would occur in space.

Accurate atomic oxygen simulation testing may require consideration of ram and sweeping exposure, synergistic effects with temperature and u.v. radiation. The degree to which flux acceleration can be achieved without generating alternative degradation mechanisms also has to be accounted for. The compromises involved in accurate simulation such as improper oxygen atom energy, enhanced flux, reactions of ions

instead of atoms, environmental gases in quantities dissimilar to that in space, metastable species effects and plasma effects are in need of definition.

Many techniques have been used to produce oxygen atoms or ions with or without acceleration for impingement on test samples. An ideal laboratory test and simulation system would provide a pure, well collimated beam of neutral oxygen atoms with a kinetic energy of 5 eV (8 km s^{-1}). Apparently, no such system exists at this time. Nearly all neutral atom test methods which have been developed or are being developed fall into one of the following categories [14]: (i) *thermal atom sources*: oxygen atoms are generated by radio frequency (RF) or microwave discharge to produce high atomic oxygen concentrations at thermal or near thermal energies; (ii) *plasma torch and atom beam sources*: oxygen atoms are generated in a high-temperature plasma, then free jet or supersonic expansion converts sensible heat to velocity. Atom energies of 1–2 eV (possibly 4 eV) have been achieved; (iii) *ion beam methods*: positive or negative atomic ion beams are produced, accelerated and focused to proper velocity, then neutralized to give a nominal 5 eV oxygen atom beam; (iv) *laser-sustained plasma atomic beam sources*: lasers are used to produce high-temperature/high-pressure plasmas which expand as free jets or supersonic beams. Atom kinetic energies of 1–12 eV have been reported with atom fluxes of 10^{15}–10^{18} atoms cm^{-2} s^{-1}.

In an attempt to establish the factors that are important for the simulation of the LEO atomic oxygen environment, Banks *et al.* [11] at NASA-Lewis, Cleveland have studied the erosion yield of Kapton© HN polyimide, fluorinated ethylene–propylene copolymer and graphite in different simulation facilities. Their study revealed that, except for graphite, the erosion yields obtained in different simulation facilities are higher than those observed in space.

There appears to be no facility which exactly simulates the LEO atomic oxygen environment. However, the laser-sustained plasma and atomic beam systems offer the best approximations. It is reported that samples of organic materials exposed to the atomic oxygen beam at Los Alamos National Laboratory (LANL) develop carpet morphology, micron scale hillocks of material, similar to that developed in the LEO [14].

The ground simulation facility certainly serves the main purpose of identifying and obtaining preliminary evaluation data on candidate materials for the LEO environment.

Ground-based evaluation of the protective coatings for atomic oxygen involves the following studies.

4.1. Mass loss measurements

This can be done in two ways. The coating can be applied to a substrate which is not affected by atomic oxygen and the weight loss of the coating can be measured as a function of atomic oxygen effect or exposure time at a given flux. Alternatively, a substrate which is vulnerable to atomic oxygen attack can be coated with the protective coating and the ability of the coating to protect the substrate from atomic oxygen can be measured by measuring the weight loss of the coated substrate as a function of atomic oxygen effect or exposure time at a given flux.

In practice, it is convenient to calculate the effect rather than measure the flux. For calculating the effect, Kapton© is exposed to atomic oxygen along with the coated substrate and weight loss measurements are made at different time intervals. From this data, the effect F expressed in atoms cm^{-2} can be calculated by the following equation

$$F = \Delta M/A \cdot \rho \cdot E$$

where ΔM is the mass loss in grams, A is the surface area of the sample in cm^2, ρ is the density and E is the erosion yield expressed in cm^3 $atom^{-1}$.

4.2. Surface analysis

Surface analysis of the samples by SEM (scanning electron microscopy) before and after exposure to atomic oxygen shows the morphological changes which may take place at the surface: surface defects, atomic oxygen erosion, undercutting of the coating and other details such as thickness of the coating and thickness of the glassy layer that is formed on reaction with atomic oxygen. Surface analysis and depth profile analysis by XPS (X-ray photoelectron spectroscopy) give insight into the chemical changes that take place in the coating on interaction with atomic oxygen.

4.3. Optical properties

The optical properties of the organic materials can undergo considerable change as the atomic oxygen interaction with the surface may cause surface roughness. Measuring the optical properties of the coatings before and after exposure to atomic oxygen will help determine the effectiveness of the coating in protecting the substrate. Many space applications require that the optical properties of the materials used should not deteriorate with time; hence evaluation of optical properties is very important for qualifying the coating for these uses.

4.4. Thermal cycling

In the LEO environment temperature variations from -80 to 120 °C can occur [1] and over a period of 30 years (lifetime of space station), the structure is subjected to 500 000 such cycles. Hence, coatings qualified for atomic oxygen protection should be subjected to thermal cycling in the ground-based facilities to determine whether they can withstand thermal cycling.

5. Fluorinated polymers

Fluorinated polymers are in general resistant to atomic oxygen attack because oxidation of the C–F bond is endothermic. Teflon© degrades 10 times slower than polyethylene. The Long Duration Exposure Facility (LDEF), which was launched in April 1984, provided the opportunity to evaluate the effect of

atomic oxygen on FEP Teflon© (fluorinated ethylene–propylene polymer). This LDEF was in the LEO for $5\frac{3}{4}$ years. The samples experienced an atomic oxygen effect of 1.22×10^{17}–7.78×10^{21} atoms cm^{-2} depending on the position of the samples. FEP Teflon© samples were available in abundance on the LDEF because of their use as silvered Teflon© thermal blankets [15].

Post-retrieval analysis of the silvered Teflon© thermal control blanket material indicated that atomic oxygen had oxidized the FEP Teflon© at higher rates than had been predicted from previous low-effect flight data. SEM analysis of a FEP Teflon© sample that received an atomic oxygen effect of 7.78×10^{21} atoms cm^{-2} revealed that the surface had microscopic roughness due to atomic oxygen attack. Samples located on rows which received a high atomic oxygen effect showed a significant increase in diffuse reflectance, compared to those which were unexposed, or exposed to minimum atomic oxygen effect. The increase in diffuse reflectance, caused by the microscopic surface structure, produced a milky-looking diffuse-reflecting surface, as opposed to the original specular reflecting surface. However, there was little change in total reflectance between silvered Teflon© samples with high- and low-effect atomic oxygen exposure. Samples exposed to a high effect show mainly diffuse reflectance whereas samples exposed to low effect show mainly specular reflectance.

Though Teflon© is being used in several LEO space components, its end-use in atomic oxygen resistant coatings has not been widely reported. Banks *et al.* [16] reported that mixing of small amounts of fluoropolymer with SiO_2 coatings (applied by ion beam deposition) greatly increases the strain-to-failure of the coatings. Mixed films with 10–18% fluoropolymer will tolerate 4–6% strain (2–3 times higher than pure SiO_2) without brittle failure.

Fewell [17] investigated atomic oxygen interaction with films and coatings of fluorinated polyphosphazene. Polybis(trifluoroethoxy)phosphazene], fluorophosphazene elastomer and poly[(octofluoropentoxy)phosphazene coatings and films were exposed to oxygen plasma, atomic oxygen beam and atomic oxygen nozzle beam. Atomic oxygen induces the same patterns of surface structural changes in poly [(fluoroalkoxy)phosphazene] films and coatings independent of whether the atomic oxygen is produced by microwave discharge or from a beam source. Atomic oxygen beam exposures resulted in differences in the stoichiometry of polyphosphazenes compared to those which had been exposed to oxygen plasma. Atomic oxygen beams caused increased formation of oxidized nitrogen (N → O) in the polymer. XPS analysis established that atomic oxygen interactions with the polymer induce microstructural changes such as rearrangements in the phosphorus–nitrogen backbone characterized by shifts in the N_{1s} binding energy of the nitrogens, branching/crosslinking, loss of nitrogen (as much as 50%), no phosphorus loss and cleavage of some pendent groups followed by oxygen replacement. XPS showed that atomic oxygen reacts with polyphosphazenes to form P = O (bond strength of 5.63 eV) and N = O (6.28 eV). The findings of this study suggest that resistance to atomic oxygen attack is mainly a function of bond strength and structural considerations. The atomic oxygen exposure study indicated that poly[bis(trifluoroethoxy)phosphazene] films were resistant to atomic oxygen attack because of backbone rearrangements, crosslinking and formation of phosphorus–oxygen and nitrogen–oxygen bonds in the polymer.

6. Silicones

Early flight data for atomic oxygen exposure of silicones have indicated atomic oxygen erosion yields between 1 and 2 orders of magnitude lower than those of Kapton H© polyimides [18]. Since silicones develop a glassy SiO_2 surface on atomic oxygen attack, they have been widely used to protect underlying oxidizable organic materials [15]. On reaction with atomic oxygen the silicone coatings ($d \approx 1\ g\,cm^{-3}$) lose their organic components and undergo a density increase to that of amorphous SiO_2 ($d = 2.4\ g\,cm^{-3}$). Due to the density increase the coatings shrink. Local shrinkage generates a microporous structure which slows but does not stop oxidation. Macroscopic shrinkage stresses the coating, causing crack formation.

Ground-based laboratory exposure of silicones to atomic oxygen has shown protection of underlying organic materials (Fig. 6) [20]. However, silicones tends to craze upon exposure to high atomic oxygen effect (Fig. 7) [20]. Also, ground-based tests have shown that silicones exposed to atomic oxygen and vacuum u.v. radiation release polymeric scission fragments which deposit on neighbouring surfaces. On further atomic oxygen attack and vacuum u.v. illumination these fragments form a glassy, dark contaminant layer [15, 21].

The LDEF data for silicones provided the opportunity to understand more about the silicone coatings and to compare the results with the ground-based laboratory plasma ashers. All atomic oxygen exposed silicone samples examined after LDEF retrieval showed microscopic crazing or cracking. SEM

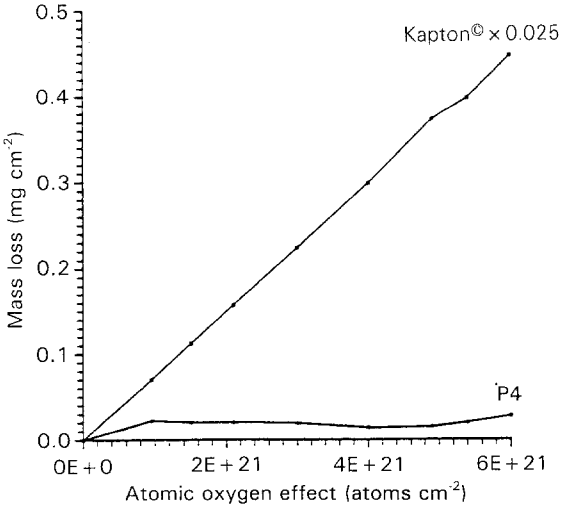

Figure 6 Mass loss of unprotected and P4 protected Kapton© on exposure to atomic oxygen (adapted from Kulig [20]).

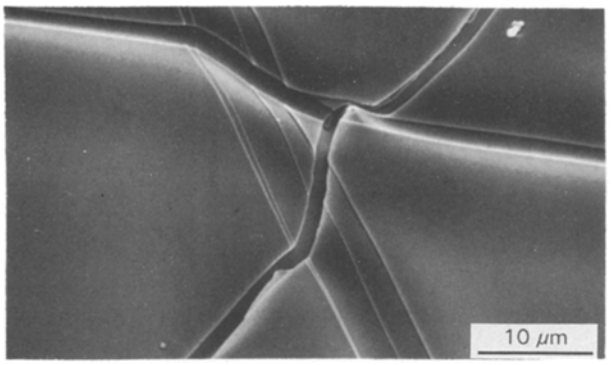

Figure 7 SEM of a crack in the P4 coating (adapted from Kulig [20]).

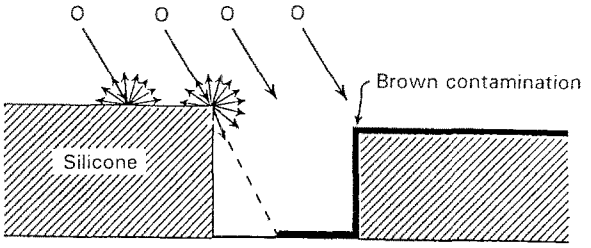

Figure 8 Section view schematic drawing of atomic oxygen attack and resulting contamination (adapted from Banks *et al.* [15]).

of silicone-coated bicycle reflectors retrieved from the LDEF showed evidence of crazing and oxidation of underlying polymeric material due to significant atomic oxygen penetration. Crazing was also observed in Kapton tape samples and in Silicone RTV 670© and Owens Illinois 650© silicones on thermal control paint surfaces on row 9.

LDEF results also indicated the presence of brown contamination on the samples located past silicone samples (Fig. 8). Brown contamination was not observed on samples which were shielded from atomic oxygen but located near silicone samples. The contamination of surfaces in the vicinity of silicone samples is due either to atomic oxygen initiated silicone polymer degradation or vacuum outgassing. However, atomic oxygen attack was necessary to produce a dark colour in the contamination layer (Fig. 8) [15]. Both LDEF results and ground-based laboratory RF plasma asher atomic oxygen interactions with silicones have indicated that brown contamination deposits can develop on adjoining surfaces. Since silicones are used in the vicinity of photovoltaic devices which rely upon high solar transmittance cover glass surfaces to maintain efficient conversion of solar energy to electrical power, contamination problems arising from silicones need to be further investigated.

7. Carborane–siloxane polymers

Though silicones form a protective SiO_2 layer on reaction with atomic oxygen, they tend to crack or craze due to volume shrinkage as discussed earlier. This problem can be overcome by incorporating carborane units into the siloxane backbone. A carborane moiety containing 10 boron atoms and will take up 15 oxygen atoms on oxidation. Hence, carborane–siloxane polymers can undergo considerable weight increase ($\sim 50\%$) on reaction with atomic oxygen, which would offset the volume shrinkage due to increase in density (from ~ 1 to $\sim 1.92\,g\,cm^{-3}$ for $B_{10}O_{15}\cdot(SiO_2)_3$).

Initially, commercially available Dexsil 300 GC© polymer (Fig. 9) was end-capped with triacetoxysilane as shown in Scheme I [20]. The acetoxy end-capped polymer (P1) reacts on exposure to moisture to form acetic acid and silanol end groups which self-condense. The curing was catalysed by dibutyl tin dioctanoate. Films were cured at room temperature and humidity for 2 days and then at 50 °C overnight. The coatings were not transparent. Optical microscope and SEM observations showed that the films tended to crystallize during curing at room temperature.

To overcome this problem, a highly functionalized polymer (P2) was synthesized by reaction of methyltriacetoxysilane and 1,7-bis(hydroxydimethylsilyl)-*m*-carborane. This produced a prepolymer with one acetoxy crosslinking site per repeat unit (Scheme II) [20] that had a polystyrene equivalent molecular

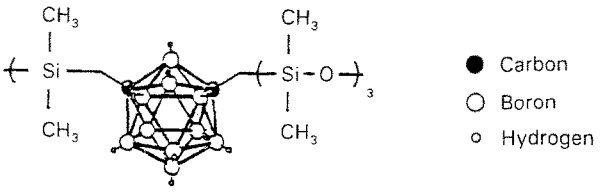

Figure 9 Poly(carborane–siloxane) [Dexil 300© GC].

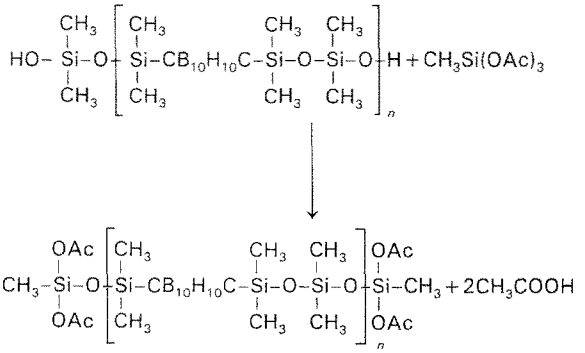

Scheme I Endcapping of Dexil 300 GC© with methyltriacetoxysilane (adapted from Kulig [20]).

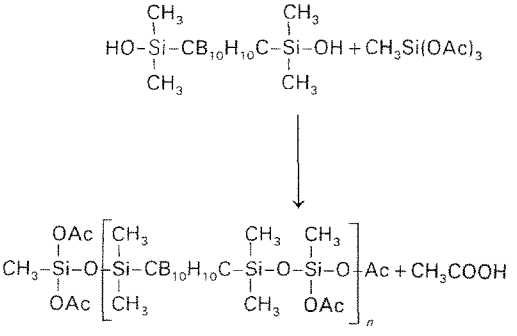

Scheme II Synthesis of P2 (adapted from Kulig [20]).

weight of 6000. (Molecular weights were calculated from a gel permeation chromatography trace that has been calibrated using polystyrene standards.) The solubility of P2 in tetrahydrofuran and toluene indicated that steric hindrance prevented the third acetoxy group from reacting. This material cures in a manner similar to P1. The P2 coatings took over 1 week to cure because of their low molecular weight.

A highly crosslinked 1.1 μm thick P2 coating on Kapton© was exposed to atomic oxygen for 1 week, a flux of atomic oxygen equivalent to 5 years of space exposure. The coated sample showed no macroscopic change in appearance and lost very little mass, whereas the uncoated 125 μm thick control became opaque and lost three quarters of its initial weight (Fig. 10) [22, 23]. The performance of an 8%PTFE/92%SiO_2 ion beam deposited coating is shown for comparison.

On exposure to plasma, coatings of P2 (on Kapton©) thinner than 1 μm stayed flat, whereas thicker ones became waffled (Fig. 11). Similar patterns have been observed in thin carbon films, caused by buckling and delamination due to high compressive stresses [24–26]. In the present case there is no evidence of delamination. The stress-relief patterns indicate that compressive stresses are present in the film and above a certain thickness can lead to waffling. At higher magnifications in the SEM a smooth, crack-free, glassy layer was observed on the film surface, with an estimated thickness of 0.15 μm. The rubbery coating can accommodate severe bending of the specimen, whereas the brittle glassy layer cracks extensively (Fig. 12) [27].

The nature of the glassy layer and its interface was investigated by X-ray photoelectron spectroscopy

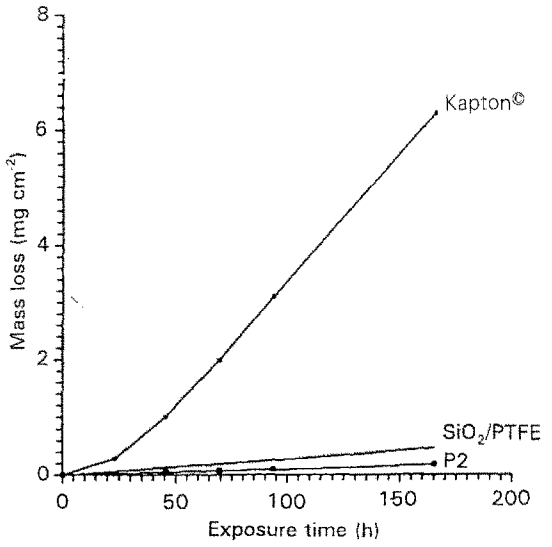

Figure 10 Mass loss of unprotected and P2 protected Kapton© on exposure to atomic oxygen (adapted from Kulig *et al.* [22, 23]).

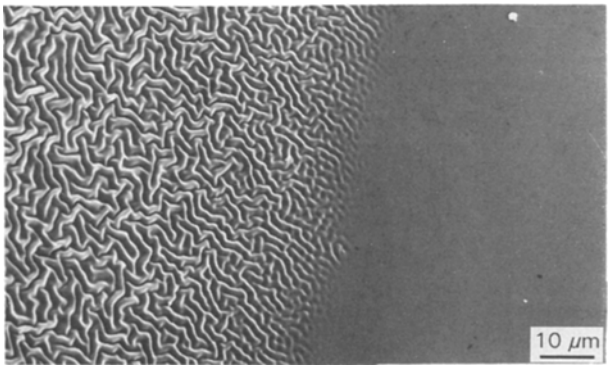

Figure 11 SEM of P2 coating on Kapton© showing waffling dependence on thickness (adapted from Kulig *et al.* [22]).

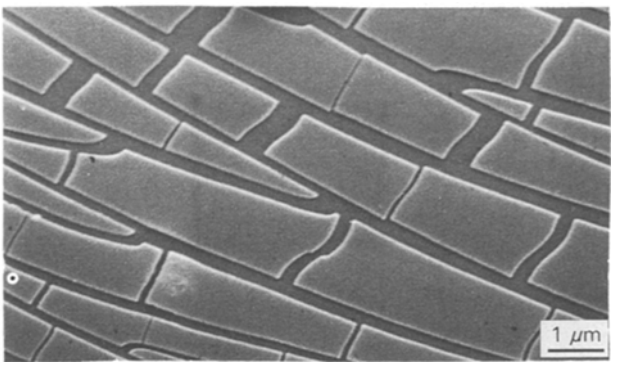

Figure 12 SEM of a broken glassy layer in a severely bent area of the P2 coating (adapted from Schwam *et al.* [27]).

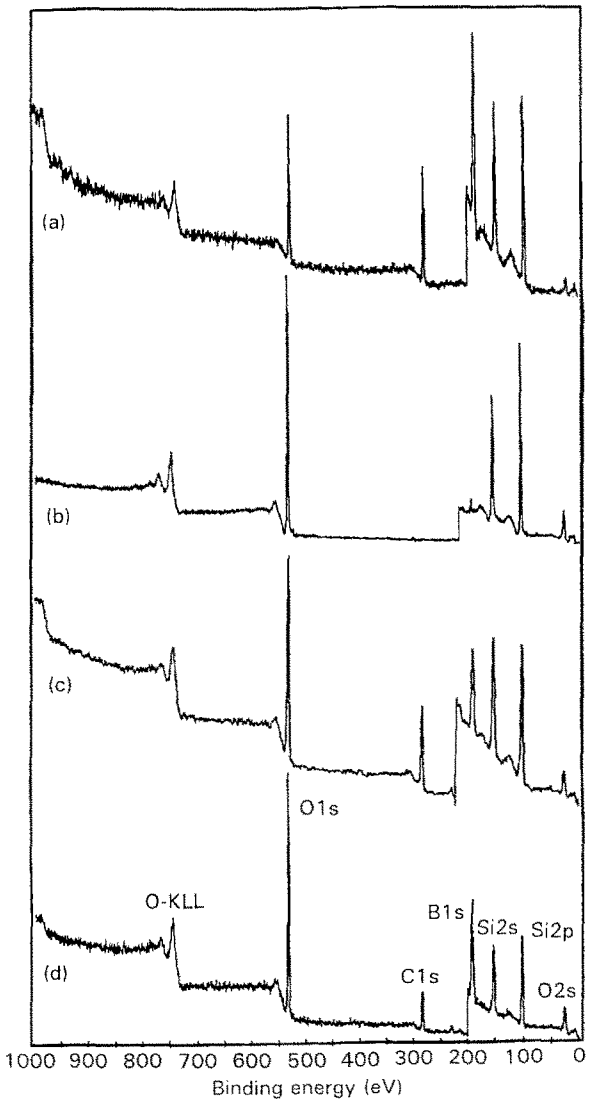

Figure 13 XPS survey spectra of P2: (a) unashed; P2 ashed for 120 h and sputtered to a depth of (b) 60 nm, (c) 160 nm, and (d) 300 nm (adapted from Schwam *et al.* [27]).

(XPS) [27]. The spectrum displayed in Fig. 13a illustrates XPS data obtained from an as-coated surface. Prior to the spectrum acquisition, 7.5 nm was sputtered from the coating to remove any adventitious contamination. As expected on the basis of the polymer composition, the XPS survey spectrum shows the presence of silicon, boron, carbon and oxygen. XPS survey spectra from a P2 coating after ashing for 120 h are shown in Fig. 13b–d in increasing depth order. At a depth of 60 nm the boron peak is very small. No carbon is present; silicon and oxygen are the major constituents. Oxidation of the surface is evident from the very prominent O(1s) peak near 530 eV in the spectrum.

At 160 nm the carbon peak appears in the spectrum and the boron peak gains height, although not reaching the value of the unashed polymer. At 300 nm the same constituents are seen. The oxygen peak is relatively high, still well above its level in the original polymer. This can be interpreted as an "oxygenated state" of the polymer. It has been proposed that the major early reaction of atomic oxygen is insertion in the C–Si bond, since that reaction generates the most energy. As this reaction increases the polymer weight and volume, it could lead to the waffling that is observed.

TABLE II Atomic concentration of P2 coating in the unashed condition and after 120 h of ashing

Condition depth (nm)	Boron	Carbon	Oxygen	Silicon
Unashed	36.8	33.5	17.1	12.7
Ashed, 60	4.1	1.8	68.0	28.2
Ashed, 300	28.2	18.4	43.6	9.8

To obtain a more quantitative evaluation of the composition changes in the P2 coatings, depth profiling scans were performed. Multiplexing for higher accuracy was performed at several depths. The results are summarized in Table II and the atomic concentrations versus depth are shown in Fig. 14. By applying non-linear curve-fitting methods to the count data, it was possible to obtain much smoother count depth profile curves [27]. From these curves the atomic ratio with respect to silicon was determined for each element (Fig. 15). Such continuous depth profile curves of the atomic ratios provide excellent insight into the possible interactions between P2 coatings and atomic oxygen. The approximate 2:1 oxygen to silicon ratio at the surface and the very low values of boron indicate that the glassy layer's top surface is close to silica composition. The mechanism of boron depletion is presumably related to exposure of the sample to humidity since boric oxide can easily hydrolyse to boric and metaboric acids. These can volatilize under the high vacuum of the XPS chamber. However, our recent studies on decaborane-based polymers show that the boron-poor surface might also be due to the contamination of the surface with SiO_2 formed by sputtering of the glass walls of the plasma asher or silicone grease contamination in the plasma asher.

The oxygen curve rises to a maximum at about 140 nm and then gradually drops, while still remaining above the original polymer composition. The maximum can be attributed to the combined contribution of the silicon and boron oxides at this depth. However, the oxygen concentration stays higher than its initial

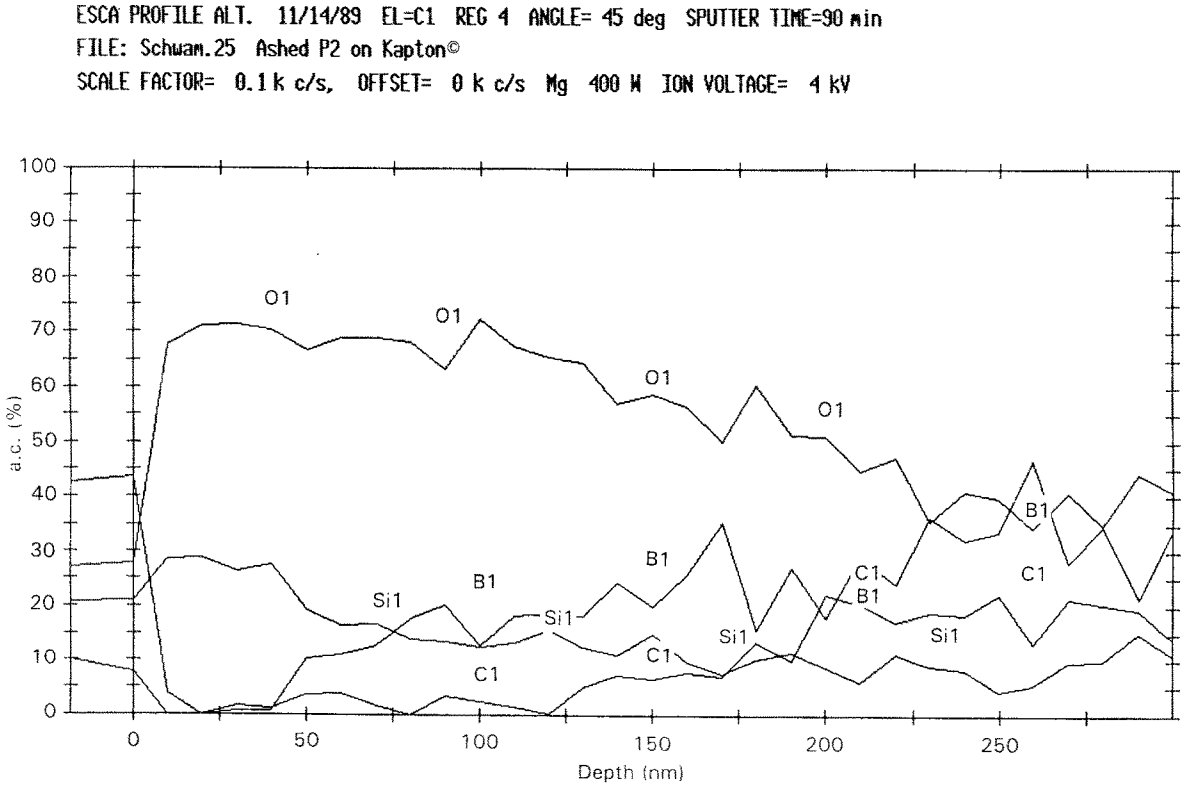

Figure 14 XPS atomic concentration depth profile for ashed P2 (adapted from Schwam *et al.* [27]).

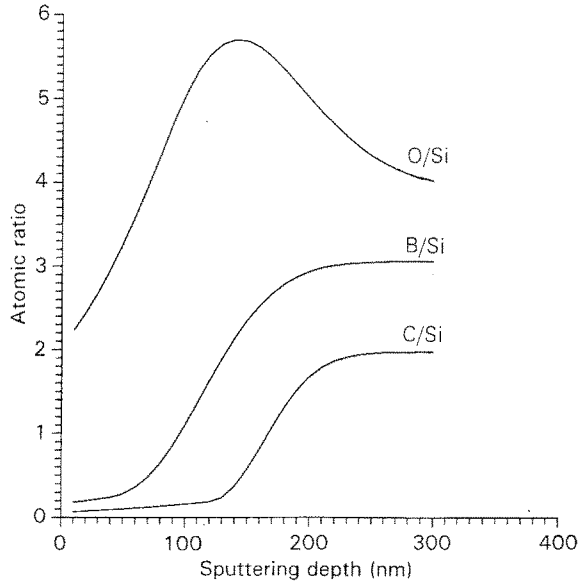

Figure 15 Atomic ratio depth profiles for a P2 coating (normalized to silicon) after 120 h of ashing (adapted from Schwam *et al.* [27]).

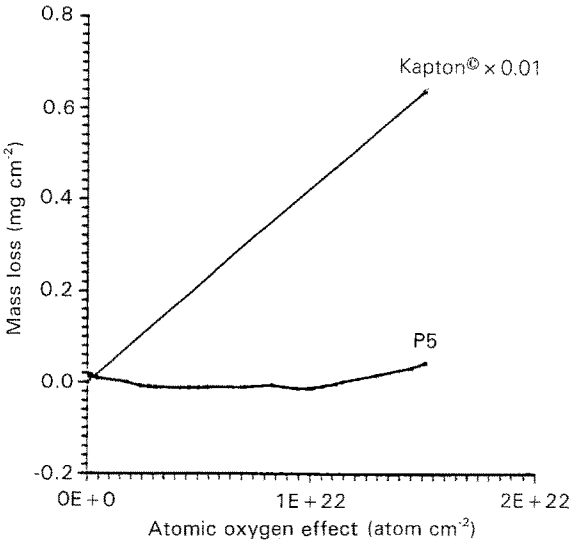

Figure 16 Mass loss of unprotected and P5 protected Kapton© on exposure to atomic oxygen (adapted from Kulig *et al.* [28]).

concentration in the polymer even at a depth of 300 nm. This explains the increase in volume, which manifests itself as waffling in the thicker regions of the coating.

Carbon is almost nil in the glassy layer and sharply increases across the interface. This in fact is the best indication of the interface location, since it is expected that practically no carbon would be present in the glassy layer. Trends in the carbon profile do not coincide with the boron curve. It is believed that the depletion of boron from the surface, perhaps by the mechanism suggested above, is a separate process independent of the glassy layer formation.

The long 1-week cure times for the moisture-cured P2 coatings prompted a search for faster cure systems. The reported curing of poly(methylhydrosiloxane) (P4) with heat and peroxides led to the development of a cure based on u.v. light generation of radicals. Poly(carborane-hydrosiloxane)s (P5) having molecular weights of 3300 and 13 000 Daltons were synthesised from bis(hydroxydimethylsilyl)-*m*-carborane by two different synthetic routes [20, 28].

Coatings of P4 and P5 were prepared by spin-coating a dilute solution of the polymer onto Kapton© substrate. Irgacure 651© was used as a photocatalyst for oxidative crosslinking of the polymers. After curing, the samples were exposed to atomic oxygen in the asher for periods ranging from 1 to 5 weeks. The u.v. cured poly(carborane–siloxane) from P5 was less susceptible to waffling than the moisture-cured coatings from P2. Waffling was observed only in very thick regions, > 2 μm, while the P2 coatings waffled at thicknesses greater than 0.7 μm. After ashing, P5 coatings were nearly smooth and featureless. In contrast, the glassy layer on oxidized P4 coatings was extensively cracked. This demonstrates the advantages of boron hydride-based polymer coatings which showed no cracking on exposure to atomic oxygen, in contrast to P4 and other silicone coatings.

Of the carborane–siloxane polymer-based coatings studied, the u.v. cured P5 coatings on Kapton© substrates provided the best protection against atomic oxygen. A Kapton© coupon coated with 0.2 μm thick P5 showed negligible mass loss after 5 weeks in the asher (Fig. 16). This is the equivalent of 22 years in the LEO. It was only after extensive ashing that the sample began to lose weight. SEM analysis showed that the edges of the sample had been damaged. It is known that the edges are more heavily attacked in the asher. Only a few areas of the coating had failed. In these regions undercutting occurred. The bulk of the damage was at the edges, so these ashing rates represent the upper limit of Kapton's mass loss rate using a P5 protective coatings.

8. Decaborane-based polymers

Though the performance of poly(carborane–siloxane)s is much superior to that of polysiloxanes and many other systems reported in the literature, the cost and the non-availability of carborane-based monomers have limited their use as protective coatings for atomic oxygen. The fact that carborane is derived from decaborane [29] prompted us to investigate the possibility of using decaborane-based polymers for the above purpose.

Decaborane ($B_{10}H_{14}$) reacts with Lewis bases (ligands, L) such as amines, phosphines, sulphides and nitriles to form adducts of the type $B_{10}H_{12}\cdot 2L$ (Scheme III) [30, 31]. When both Lewis base sites are in the same molecule, a linear polymer can be obtained. Synthesis of decaborane-based linear polymers from Lewis bases such as amines, amides, nitriles and phosphines was reported [32–37] in the early 1960s. Though these polymers were thought to be useful as high-temperature stable polymers or even as high-energy fuels, their use as boron-containing preceramic polymers was not recognized. In recent years the potential application of decaborane-based polymers as precursors for boron carbide and boron nitride has been investigated [38–47].

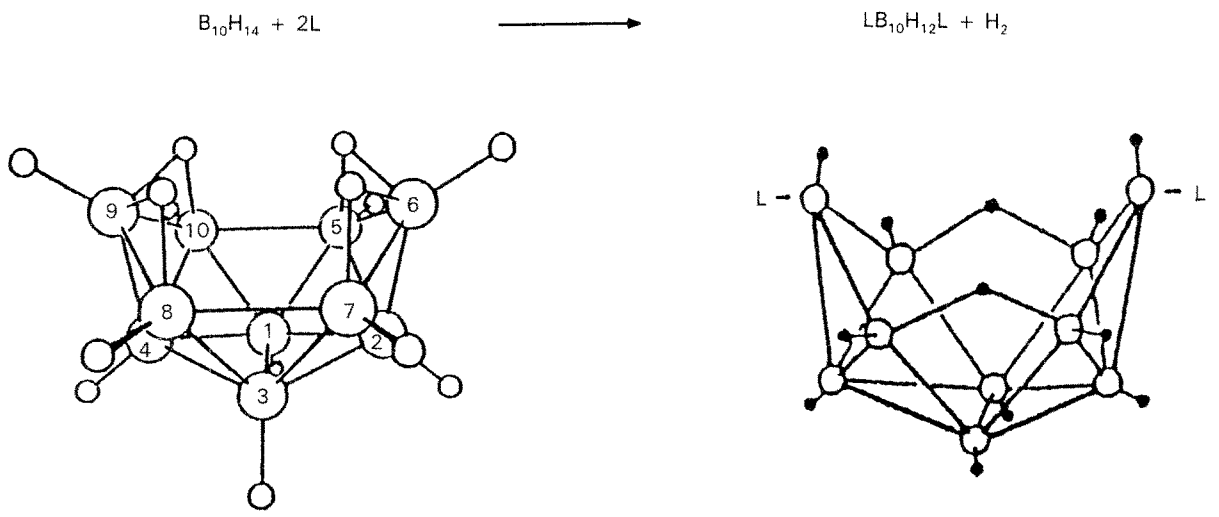

Scheme III Reaction of decarborane with Lewis bases (adapted from Niedenzu and Buschbeck [30] and Muetterties [31]).

Besides their possible end-use as preceramic polymers, decaborane-based polymers should serve as potential candidates for atomic oxygen resistant coatings since the decaborane repeat unit can take up 15 oxygen atoms, resulting in considerable weight increase. Decaborane-based polymers are soluble only in polar solvents such as dimethylacetamide, dimethylformamide and dimethylsulphoxide. Coatings from $[B_{10}H_{12}\cdot H_2NCH_2CH_2CH_2NH_2]_n$ and $[B_{10}H_{12}\cdot N(CH_3)_2CH_2CH_2N(CH_3)_2]_n$ were translucent. Atomic oxygen resistant coatings intended for application on Kapton© and on silver mirrors should be transparent. Moreover, use of polar solvents such as dimethylacetamide or dimethylformamide resulted in the formation of defect sites due to dewetting. Undercutting occurred at the defect sites due to the reaction of the substrate with atomic oxygen. In order to overcome the solubility problem and also to increase the flexibility of the polymeric chain, polymers were synthesized from diamines containing Si–O–Si or ether linkages (Scheme IV) [48, 49]. X-ray diffraction (WAXD) studies of these polymers indicated that they are amorphous. A comparison of the WAXD of $[B_{10}H_{12}\cdot H_2NCH_2CH_2CH_2NH_2]_n$ with those of DBP-3 and -4 (Fig. 17) reveals that the incorporation of ether linkage reduces the ordered structure present to some extent in the former [50]. The coating obtained from the former tends to develop cracks on bending whereas flexible coatings are obtained from polymers containing siloxane and ether linkages.

The polymer (DBP-1) obtained from 1,3-bis(3-aminopropyl)-1,1,3,3-tetramethyldisiloxane was soluble in tetrahydrofuran and in polar solvents. The polymers containing ether linkages (DBP-2,3,4) were insoluble in tetrahydrofuran but were soluble in a 1 : 1 mixture of tetrahydrofuran and dimethylacetamide or dimethylformamide.

On reaction with atomic oxygen, coatings derived from decaborane-based polymers are expected to generate a protective layer of boric oxide on their surfaces that prevents further oxidation of the substrate. It was of interest to investigate the atomic oxygen resistance of DBP-1 as it is soluble in tetrahydrofuran. 125 μm thick Kapton© film was the substrate. Circular Kapton© coupons of 1.5 cm dia. were spin-coated with a 20% solution of DBP-1 on one side and gold-coated on the other side. They were dried in an air oven at 38 °C for 10 h and then under vacuum at 60 °C for 24 h. Polymer-coated Kapton© coupons and the control Kapton© coupon (gold-coated on one side) were exposed to atomic oxygen in the plasma asher. Weight loss measurements were taken at different time intervals.

There was practically no weight loss observed on exposure to atomic oxygen for the Kapton© coupon coated with DBP-1 (Fig. 18) [49]. SEM studies of the

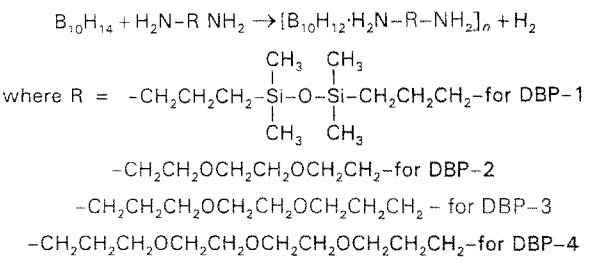

Scheme IV Synthesis of decaborane-based polymers (adapted from Packirisamy *et al.* [49]).

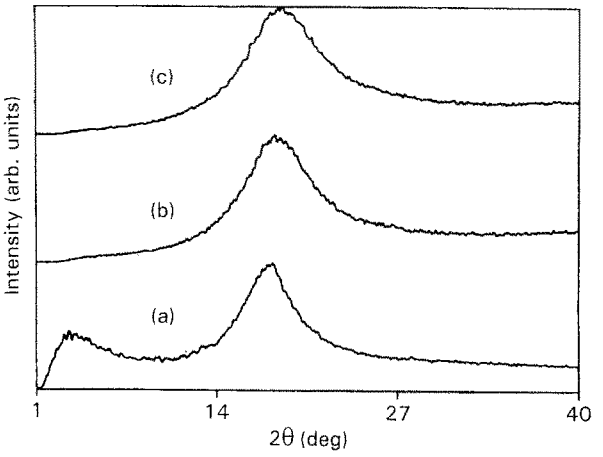

Figure 17 X-ray diffraction patterns of (a) $[B_{10}H_{12}\cdot H_2NCH_2CH_2CH_2NH_2]_n$, (b) DBP-3 and (c) DBP-4 (adapted from Packirisamy *et al.* [50]).

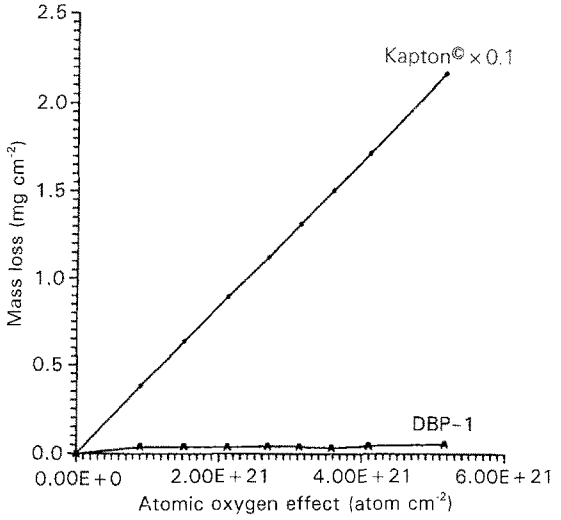

Figure 18 Mass loss of unprotected and DBP-1 protected Kapton© on exposure to atomic oxygen (adapted from Packirisamy *et al.* [50]).

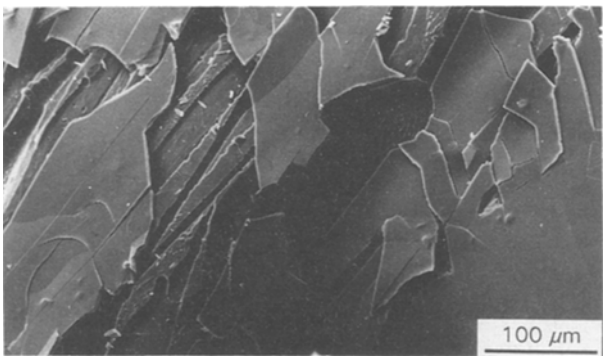

Figure 19 SEM of broken glassy layer of DBP-1 coating ashed for 624 h (adapted from Packirisamy *et al.* [50]).

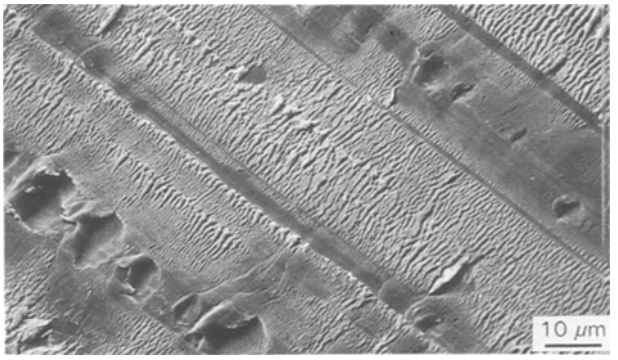

Figure 20 SEM of polymer layer underneath the glassy layer in DBP-1 coating ashed for 624 h (adapted from Packirisamy *et al.* [50]).

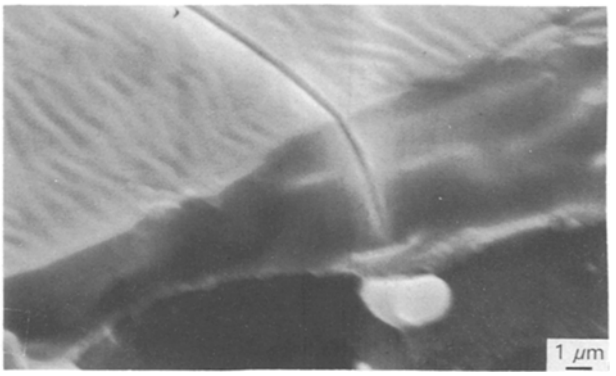

Figure 21 SEM of a crack obtained by severe bending of DBP-1 coating exposure to atomic oxygen (adapted from Packirisamy *et al.* [50]).

coatings exposed to atomic oxygen for 624 h show that the surface had no defects and the Kapton© was completely protected. In order to understand more about the coating after exposure to atomic oxygen, it was scraped and analysed by SEM. Fig. 19 shows the broken glassy layer and Fig. 20 shows the underlying flexible polymer [51].

Contamination of the space components by degradation products of silicone coatings is of great concern. Thus, it was desirable to investigate the decaborane based polymers derived from diamines containing only ether linkages. The suitability of DBP-2, -3 and -4 polymers as atomic oxygen resistant coatings was studied. As these polymers were insoluble in pure tetrahydrofuran, a solvent mixture of tetrahydrofuran and dimethylacetamide was used to apply the coating. This eliminated the dewetting problem mentioned earlier. Coatings obtained from DBP-2 and DBP-3 were translucent and coatings from DBP-4 were transparent.

The atomic oxygen resistance of DBP-4 coatings was evaluated following the procedure described for DBP-1. Considerable weight loss was observed on exposure to atomic oxygen for DBP-4 coated Kapton© when compared to DBP-1 coated Kapton©. The mass loss data suggest that the performance of DBP-1 is better than that of DBP-4. However, SEM studies of the former indicated that DBP-4 offered very good protection to the substrate and the weight loss was mainly due to undercutting at a defect site.

SEM studies of cracks (Fig. 21) developed by severe bending of DBP-1 and DBP-4 coatings exposed to atomic oxygen indicate that a crack generated in the glassy layer propagates deep into the underlying polymer, suggesting that the coatings have poor mechanical properties when compared to poly(carborane–siloxane) systems. As discussed earlier, severe bending of the poly(carborane–siloxane) coating (P2) exposed to atomic oxygen resulted in the development of extensive cracks in the glassy layer but no cracks were observed in the polymeric coating beneath the glassy layer (Fig. 12). Coatings based on poly(carborane –siloxane) are crosslinked systems and hence have better mechanical properties. The decaborane based polymers made up to now have low molecular weights and undergo degradation in polar solvents. These could be the reasons for their poor mechanical properties.

XPS depth profile analysis of the DBP-4 coating showed the presence of a 20 nm thick SiO_2 layer. Since this polymer does not contain Si, the deposition of SiO_2 over the oxidized coating might be due to the sputtering of the glass walls of the plasma asher by plasma.

9. Conclusions

A review of the literature on atomic oxygen resistant coatings suggests that significant advances have been made over the last 10 years in the area of ground-based simulation facilities for studying the atomic oxygen resistance of the coatings and on the development of different inorganic and polymeric coating systems. Polymer-based coatings offer several advantages over inorganic coatings. There appear to be three classes of polymeric materials which can be used as atomic oxygen resistant coatings: (i) carbon backbone polymers which degrade at a slower rate in atomic oxygen than conventional polymers (e.g. Teflon©), (ii) polymers which stabilize by reacting with atomic oxygen (e.g., fluorinated polyphosphazenes), and (iii) inorganic and semi-inorganic polymers which react with atomic oxygen to form a glassy oxide layer that prevents further reaction of the coatings with atomic oxygen. The flexible polymer beneath the glassy layer allows the coating to heal if the glassy layer is damaged and also improves the adhesion of the glassy layer to the substrate.

Ground-based evaluation of different polymeric systems suggests that poly(carborane–siloxane)s are by far the best. However, the high cost and non-availability of carborane–siloxane monomers limit their potential. As boron hydride-based polymers offer the advantage of incorporating large amounts of boron into the polymer backbone, a number of decaborane-based polymers were developed in an attempt to replace the poly(carborane–siloxane)s. Though these polymers offer protection to atomic oxygen, analysis of the coatings exposed to atomic oxygen reveals that the coatings have poor mechanical properties. Poly(carborane–siloxane) polymeric coatings are crosslinked systems and hence they provide better mechanical properties whereas decaborane-based polymers are not crosslinkable. Decaborane-based polymers are soluble only in polar solvents, in which they degrade. This is probably one of the reasons for the poor mechanical properties of these coatings. The siloxane-linkage containing decaborane polymer is promising due to the polymer solubility in tetrahydrofuran, hence problems associated with the degradation of decaborane-based polymers in polar solvent can be avoided. However, considerable research is necessary for the synthesis of high molecular weight, stable, crosslinkable polymers of this type.

There appear to be no reports on the use of other preceramic polymers as atomic oxygen resistant coatings. It would be worthwhile to focus attention on preceramic polymers with oxidative yields $> 100\%$. Since activity in the LEO will increase as commercialization of space proceeds, it is anticipated that there will be increasing demand for protective coatings for space structures used in the LEO. Research needs to be focused on cost-effective synthetic procedures for developing polymeric materials with high oxidative yields.

Acknowledgement

This work was supported by NASA-CCDS, Case Western Reserve University, Cleveland. One of the authors (S. P.) is thankful to the Indian Space Research Organization for granting him leave of absence.

References

1. R. CULL, Paper 55, presented at the Rubber Division Meeting, American Chemical Society, Dallas, Texas, April 1988, p. 11.
2. L. LEGER, AIAA 21st Aerospace Sciences Meeting, Paper No. 83-0073, January 1983.
3. A. F. WHITAKER, *ibid.*, Paper No. 83-2632, October 1983.
4. W. S. SLEMP, B. SANTOS and G. F. SYKES, AIAA Paper No. 85-0421, 1985.
5. D. G. ZIMCIK, R. C. TENNYSON, L. J. KOK and C. R. MAAG, in Proceedings of the Third European Symposium on Spacecraft Materials in Space Environment, ESA SP-232, Noordwijk, Netherlands, October 1985.
6. D. McCLURE, NASA Contractors Report 4158, p. 28 (1988).
7. C. K. PURVIS, NASA/SDIO Space Environmental Effects on Materials Workshop, Hampton, VA, USA, June–July 1988. NASA Conference Publication 3035, Part 1, pp. 5–24.
8. D. E. BOWLES and D. R. TENNEY, *SAMPE J.* May/June (1987) 49.
9. J. VISENTINE, NASA/SDIO Space Environmental Effects on Materials Workshop, Hampton, VA, USA, June–July 1988. NASA Conference Publication 3035, Part 1, pp. 179–195.
10. D. TENNY, *ibid.*, p. 29.
11. B. A. BANKS, S. K. RUTLEDGE and J. A. BRADY, Paper presented at the 15th Space Simulation Conference, Williamsburgh, VA, USA, October–November 1988.
12. B. A. BANKS, S. K. RUTLEDGE, J. A. BRADY and J. E. MERROW, NASA/SDIO Space Environmental Effects on Materials Workshop, Hampton, VA, June–July 1988. NASA Conference Publication 3035, Part 1, pp. 197–239.
13. B. A. BANKS and S. K. RUTLEDGE, Paper presented at the 4th International Conference on Spacecraft Materials in Space Environment, CERT, Toulouse, France, September 6–9 1988.
14. S. L. KOONTZ, NASA/SDIO Space Environmental Effects on Materials Workshop. NASA Conference Publication 3035, Part 1, pp. 241–253 (1988).
15. B. A. BANKS, L. GEBAUER and C. M. HILL, Paper presented at the 1st LDEF Post-Retrieval Symposium, Kissimmee, FL, June 2–8 1991.
16. B. A. BANKS, S. K. RUTLEDGE, K. K. DE GROH, C. LAMOREAUX and R. OLLE, Paper presented at the Society of Vacuum Coater, 35th Annual Technical Conference, Baltimore, MD, USA, March 1992.
17. L. L. FEWELL, *J. Appl. Polym. Sci.* **41** (1990) 391.
18. B. A. BANKS, S. K. RUTLEDGE, P. E. PAULSEN and T. J. STUEBER, NASA TM 101971 (1989).
19. "CRC Handbook of Chemistry and Physics", 160th Edn, edited by R. C. Weast (CRC Press Inc., Boca Raton, FL, 1979–1980) p. F-80.
20. J. KULIG, MS thesis, Case Western Reserve University, Cleveland (1991).
21. B. A. BANKS, S. K. RUTLEDGE, K. K. DE GROH, M. J. MIRTICH, L. GEBAUER, R. OLLE and C. M. HILL, Paper presented at the 5th International Symposium on Materials in Space Environment, Cannes-Mandelieu, France, September 16–20 1991.
22. J. KULIG, D. SCHWAM and M. H. LITT, in "Inorganic and Metal Containing Polymeric Materials", edited by J. Sheats (Plenum Press, New York, 1990) pp. 225–232.
23. J. KULIG, G. JEFFERIS and M. H. LITT, *Polym. Prep.* **61** (1989) 219.
24. D. NIR, *Thin Solid Films* **112** (1984) 41.
25. G. GILLE and B. RAU, *ibid.* **120** (1984) 109.
26. N. MATUDA, S. BABU and A. KINBARA, *ibid.* **81** (1981) 301.
27. D. SCHWAM, J. KULIG and M. H. LITT, *Chem. Mater.* **3** (1991) 616.
28. J. KULIG, D. SCHWAM and M. H. LITT, to be published.
29. R. N. GRIMES, "Carboranes" (Academic Press, New York, 1970) pp. 54–55.

30. "Gmelin Handbook of Inorganic Chemistry", 8th Edn, Vol. 54, edited by K. Niedenzu and K.-C. Buschbeck (Springer, Berlin, 1979) pp. 151–165.
31. "Boron Hydride Chemistry", edited by E. L. Muetterties (Academic Press, New York, 1975) pp. 136–137.
32. H.-J. SCHROEDER, J. R. REINER and T. L. HEYING, *Inorg. Chem.* **1** (1962) 618.
33. H.-J. SCHROEDER, J. R. REINER, T. A. KNOWLES, *ibid.* **2** (1963) 393.
34. J. R. REINER and H.-J. SCHROEDER, US Patent 3 141 856 (1964).
35. H.-J. SCHROEDER, US Patent 3 155 630 (1964).
36. G. W. PARSHALL, US Patent 3 035 949 (1962)
37. J. GREEN, M. M. FEIN, N. MEYES, G. DONOVAN, M. ISRAEL and M. S. COHEN, *J. Polym. Sci., Polym. Lett. Ed.* **2** (1984) 987.
38. D. SEYFERTH, W. S. REES, Jr., A. LIGHTFOOT, J. S. HAGGERTY, *Chem. Mater.* **1** (1989) 54.
39. W. S. REES, Jr and D. SEYFERTH, *Ceram. Eng. Sci. Proc.* **9** (1988) 1009.
40. A. LIGHTFOOT, W. S. REES, Jr. and J. S. HAGGERTY, *ibid.* (1988) 1021.
41. D. SEYFERTH, and W. S. REES, Jr., *Chem. Mater.* **3** (1991) 1106.
42. W. S. REES and D. SEYFERTH, *Ceram. Eng. Sci. Proc.* **10** (1989) 837.
43. R. E. JOHNSON, US Patent 4 832 895 (1989).
44. R. E. JOHNSON, US Patent 4 810 436 (1989).
45. R. E. JOHNSON, US Patent 4 931 100 (1990).
46. D. SEYFERTH and W. S. REES, Jr., US Patent 4 871 826 (1989).
47. W. S. REES, Jr and D. SEYFERTH, *J. Amer. Ceram. Soc.* **71** (1988) C194.
48. S. PACKIRISAMY and M. H. LITT, Paper presented at Materials in Space Meeting, Cleveland, May 1992.
49. S. PACKIRISAMY, D. SCHWAM and M. H. LITT, *Polym. Prepn.* **34/2** (1993) 197.
50. S. PACKIRISAMY, D. SCHWAM and M. H. LITT, to be published.
51. S. PACKIRISAMY and M. H. LITT, to be published.

Received 5 January
and accepted 19 May 1994